

The variability plane of accreting compact objects

E. G. Körding,¹* S. Migliari,² R. Fender,¹ T. Belloni,³ C. Knigge¹ and I. McHardy¹

¹*School of Physics and Astronomy, University of Southampton, Hampshire SO17 1BJ*

²*Centre for Astrophysics and Space Sciences, Code 0424, University of California at San Diego, La Jolla,*

³*INAF-Osservatorio Astronomico di Brera, Via E. Bianchi 46, I-23807 Merate (LC), Italy*

Accepted 2007 June 5. Received 2007 May 29; in original form 2007 March 7

ABSTRACT

Recently, it has been shown that soft-state black hole X-ray binaries and active galactic nuclei populate a plane in the space defined by the black hole mass, accretion rate and characteristic frequency. We show that this plane can be extended to hard-state objects if one allows a constant offset for the frequencies in the soft and the hard state. During a state transition, the frequencies rapidly move from one scaling to the other depending on an additional parameter, possibly the disc fraction. The relationship among frequency, mass and accretion rate can be further extended by including weakly accreting neutron stars (NSs). We explore if the lower kHz quasi-periodic oscillations of NSs and the dwarf nova oscillations of white dwarfs can be included as well and discuss the physical implications of the found correlation.

Key words: accretion, accretion discs – black hole physics – galaxies: active – X-rays: binaries.

1 INTRODUCTION

The general idea that X-ray binaries (XRBs) and active galactic nuclei (AGN) have similar central engines, if scaled with black hole mass, is increasingly supported by empirical correlations connecting both classes. First, the fundamental plane of accreting black holes connects XRBs and AGN through a plane in the black hole mass, radio and X-ray luminosity space (Merloni, Heinz & Di Matteo 2003; Falcke, Körding & Markoff 2004). Recently, McHardy et al. (2006) have reported that a second plane connecting stellar and supermassive black holes exist in the space defined by the accretion rate, the black hole mass and a characteristic time-scale of the X-ray variability. This suggests that all black holes can be unified by taking the accretion rate as well as the black hole mass into account. Here, we explore the latter correlation in further detail and discuss the inclusion of strongly sub-Eddington black holes (BHs) and neutron stars (NSs).

The power spectral density (PSD) of NS and BH XRBs can be well described by a number of Lorentzians with variable coherence factor Q (e.g. Psaltis, Belloni & van der Klis 1999; Belloni, Psaltis & van der Klis 2002b). Each Lorentzian is described by their characteristic frequency (the frequency of the maximum of the Lorentzian in the frequency times power plot). As presented in Belloni et al. (2002b), it is possible to fit NSs and BHs with the following.

(i) A zero-centred low-frequency Lorentzian L_{lb} fitting the low-frequency end of the band-limited noise with characteristic frequency ν_{lb} . Usually, this frequency is denoted as ν_{b} in the literature.

However, to avoid the confusion with the break frequency studied in AGN, we add the prefix ‘l’ for low.

(ii) Two Lorentzians fitting (LF) the high-frequency end of the band-limited noise with frequencies ν_1 and ν_u (the lower and the upper high-frequency Lorentzian L_1 and L_u). These two Lorentzians take over the role of the upper and the lower kHz quasi-periodic oscillation (QPO) if they are present.

(iii) One or two Lorentzians fitting the region around the frequency of the low-frequency QPO. The narrow core of the QPO (L_{LF}) has the characteristic frequency ν_{LF} , while the broader ‘hump’ Lorentzian L_{h} has a characteristic frequency ν_{h} .

For a sketch showing the different Lorentzians, see Fig. 1.

XRBs are observed in several states: the hard, the soft and the intermediate state (IMS). For definitions, subclasses and examples see, for example, Nowak (1995), Belloni et al. (2005) and Homan & Belloni (2005), but see also McClintock & Remillard (2006) for slightly different definitions.

The measured shapes of AGN PSDs are similar to those of soft-state XRBs (see e.g. McHardy 1988; Markowitz et al. 2003). The time-scales for AGN are several orders of magnitudes longer, roughly in agreement with the expectation that all length-scales increase linearly with black hole mass. The uncertainties of the measured AGN PSDs are usually too large to fit a detailed Lorentzian model (but see I. M. McHardy et al., in preparation), due to the long time-scales. Thus, one uses broken power-law models. The shape of the PSD of AGN and XRBs at high Fourier frequencies is well described by a power law with index ~ -2 (e.g. Green, McHardy & Lehto 1993; Cui et al. 1997). For Seyfert galaxies and those soft-state XRBs similar to Cyg X-1 the PSD at low Fourier frequencies turns to a power law with index ~ -1 (see Fig. 1, Cui et al. 1997;

*E-mail: Elmar@phys.soton.ac.uk

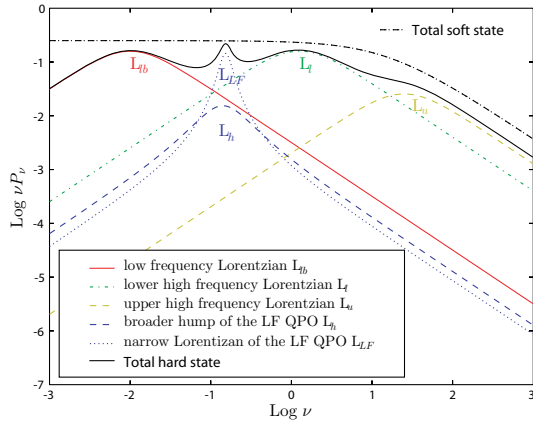


Figure 1. Sketch of the different Lorentzians found in BH and NS XRBs. The x -axis denotes the frequency and on the y -axis we show frequency times power. Besides the Lorentzians found in hard-state objects, we also show a broken power-law model found for the PSDs of soft-state BHs. We have increased the normalization of the soft-state model so that it lies above the model for the hard state.

Edelson & Nandra 1999; Uttley, McHardy & Papadakis 2002). The Fourier frequency of the turnover will be denoted as the high break frequency ν_{hb} . Using the bolometric luminosity as a tracer for the accretion rate, McHardy et al. (2006) found that this high break frequency is related to the accretion rate and black hole mass as $\nu_{\text{hb}} M \propto \dot{M} / \dot{M}_{\text{Edd}}$ for soft-state objects.

It has recently been found by Migliari, Fender & van der Klis (2005) that for the BH GX 339–4 the frequency of the lower high-frequency Lorentzian ν_l and for the NS 4U 1728–34 the frequency of the ‘hump’-Lorentzian ν_h is correlated with the radio luminosity in their hard state as $\nu_{l,h} \propto L_{\text{R}}^{0.7}$, where $\nu_{l,h}$ denotes either ν_l or ν_h . As the radio luminosity is a good tracer of the accretion rate (Körding, Fender & Migliari 2006b, $L_{\text{R}} \propto \dot{M}^{1.4}$), the correlation can be written as $\nu_{l,h} \propto \dot{M}$. It is therefore suggestive that the ‘variability plane’ found for high-state XRBs and AGN can be extended to hard-state BHs or even NSs.

As shown in Fig. 1, the superposition of the different Lorentzians (L_{lb} , L_{h} , L_{l} and L_{u}) creates a flat plateau in the νP_{ν} plots, and the PSD can therefore be roughly described with power law with index ~ -1 for frequencies between ν_{lb} and ν_l . This power law steepens to a power law with index ~ -2 at the peak of the high-frequency Lorentzians (L_{l} and L_{u}), similar to the behaviour found in soft-state XRBs and AGN. It is therefore likely that the frequency of either the upper or the lower high-frequency Lorentzian (ν_{u} or ν_l) corresponds to the high break frequency found in soft-state XRBs and AGN. The lower high-frequency Lorentzian L_{l} usually dominates the high-frequency end of the band-limited noise (e.g. Pottschmidt et al. 2003). Additionally, ν_l and ν_{u} are not linearly coupled (e.g. Belloni et al. 2002b). While the frequency of the lower high-frequency Lorentzian ν_l seems to be proportional to \dot{M} , ν_{u} is therefore not linearly proportional to \dot{M} for individual sources. This suggests that the lower high-frequency Lorentzian L_{l} with the characteristic frequency ν_l corresponds to the high break frequency of AGN.

We note that for NS one observes ‘parallel tracks’ for kHz QPOs on frequency flux diagrams (e.g. Ford et al. 2000; van der Klis 2001), that is, while flux and frequencies are strongly correlated for short periods of time, the correlation is nearly absent for longer time-scales. If the X-ray luminosity (flux) is a good tracer of the accretion rate, there cannot be a simple one-to-one dependence of

the frequency ν_l of the lower high-frequency Lorentzian on accretion rate. However, there are at least three possible tracers of the accretion rate (frequencies, X-ray luminosity and radio luminosity) and the frequencies or the radio luminosity might be better indicators than the X-ray luminosity.

Psaltis et al. (1999) and Belloni et al. (2002b) present a correlation of the frequencies of the lower kHz QPO with those of the low-frequency QPO ν_{LF} . This correlation can be extended to include noise features of black hole XRBs (BHXRBS) by using the lower high-frequency Lorentzian L_{l} as the lower kHz QPO. Also cataclysmic variables (CVs) can be included by using dwarf nova oscillations (DNOs, e.g. Warner, Woudt & Pretorius 2003) and the QPO frequency. Here, we explore if the variability plane found in sort-state AGN and XRBs can also be extended to hard-state BH XRBs and NSs or even to white dwarfs (WDs).

2 THE SAMPLE

To explore the dependence of the variability properties on the accretion rate and mass of the compact object, we construct a sample of hard- and soft-state BHs and NSs with estimated accretion rates.

2.1 Accretion rates

Soft-state BHs and all NSs are generally assumed to be efficiently accreting. Thus, we can use the bolometric luminosity directly as a measure of the accretion rate:

$$\dot{M} = \frac{L_{\text{bol}}}{0.1c^2}, \quad (1)$$

where we assumed an accretion efficiency of $\eta = 0.1$.

For hard-state BHs the accretion rate is not linearly related to the X-ray as the accretion flow is likely to be inefficient (e.g. Esin, McClintock & Narayan 1997). However, Körding et al. (2006b) provide estimates of the accretion rates from either radio or X-ray luminosities. The accretion measure based on the radio luminosity is

$$\dot{M} = 3 \times 10^{17} \left(\frac{L_{\text{Rad}}}{10^{30} \text{ erg s}^{-1}} \right)^{12/17} \text{ g s}^{-1}. \quad (2)$$

In the notation given in Körding et al. (2006b), we have set $f = 1$ and $\eta = 0.1$ to allow for a direct comparison between hard-state BHs and sources with a measured accretion rate obtained from the bolometric luminosity. Using the fundamental plane of accreting BHs (and the radio/X-ray correlation for XRBs) the radio luminosity accretion measure can be translated to an accretion rate estimate based on the 2–10 keV X-ray luminosity:

$$\dot{M} \approx 3.4 \times 10^{17} \left(\frac{L_{2-10 \text{ keV}}}{10^{36} \text{ erg s}^{-1}} \right)^{0.5} \left(\frac{M}{M_{\text{GX339}}} \right)^{0.43} \text{ g s}^{-1}. \quad (3)$$

We note that this accretion measure does depend not only on the X-ray luminosity but also on the mass of the BH. While the masses of BH XRBs are typically around $\sim 10 M_{\odot}$, this mass-term provides an additional uncertainty compared to the accretion rate measure based on the radio luminosity. Thus, we will estimate the accretion rate from the radio luminosity if quasi-simultaneous measurements of the radio flux and the timing features are available. Otherwise, we have to use the X-ray flux to obtain an accretion rate estimate.

The uncertainty of these accretion rate measures is hard to access as there are only a few data points available to normalize the accretion measure. The sample standard deviation of the four BH data points is ~ 0.3 dex, but has little significance. If one includes also the

NS points (overall 14 points), we find a scatter of ~ 0.2 dex. Another possibility to measure the uncertainty of the accretion measure is via the fundamental plane of accreting BHs. If both accretion measures (based on the radio and the X-ray emission) presented here are exact, there would be no scatter in radio/X-ray correlation found for XRBs and the fundamental plane for XRBs and AGN. The scatter around the fundamental plane can therefore be used as rough estimator of the uncertainty of the accretion rate measure. The cleanest sample for the fundamental plane including only hard-state XRBs and low-luminosity AGN has a scatter of 0.15 dex (Körding, Falcke & Corbel 2006a). This suggests that the uncertainties of the accretion rate measure based on radio luminosity is around ~ 0.2 dex. The accretion rate measure based on the X-ray luminosity will have a similar intrinsic uncertainty, but has additional uncertainties due to uncertainties of the BH mass estimates.

The accretion rate measure based on the radio luminosity is also applicable to island-state NS. However, as the radio luminosity accretion rate measure has been normalized using accretion rates obtained from bolometric luminosities its absolute accuracy is unlikely to exceed the measure based on bolometric luminosities for efficiently accreting objects. In summary, we will use the following accretion rate measures in order of preference.

- (i) Accretion rates from bolometric luminosity for soft-state BHs and NSs.
- (ii) Accretion rates estimated from the radio luminosity for hard-state BHs.
- (iii) Accretion rates estimated from the X-ray luminosity for hard-state BHs.

Throughout this paper, we will measure the accretion s^{-1} , all frequencies in Hz and masses of compact objects in solar masses.

2.2 Black holes

Our hard-state BH sample is based on the measurements in the public *RXTE* archive as well as already published data. We select all sources which have well measurable frequencies ν_1 as well as estimates for the black hole mass and distance. However, in order to obtain an estimate of ν_1 one needs a hard-state power spectrum, since in the hard-intermediate state characteristic frequencies are higher and the broad lower high-frequency Lorentzian (L_1) cannot usually be detected (with the exception of GRS 1915+105). Moreover, the source count rate needs to be sufficiently high to allow a detection. This rules out the final parts of the outbursts and limits our sample to bright early hard-state observations. Unfortunately, only few sources have been observed sufficiently early in their outburst to fulfil all the requirements are as follows:

(i) *GX 339–4*. Migliari et al. (2005) present values for ν_1 and the radio fluxes of *GX 339–4* in its hard state. These radio fluxes have been used to estimate the accretion rate. The distance to *GX 339–4* is still uncertain, Shahbaz, Fender & Charles (2001) and Jonker & Nelemans (2004) give a lower limit of 6 kpc, but the distance may be as high as 15 kpc (Hynes et al. 2004). We therefore adopt a distance of 8 kpc. The mass function is $5.8 \pm 0.5 M_{\odot}$ (Hynes et al. 2003), which is therefore a lower limit for the mass of the BH. If one assumes zero mass for the companion and a mean inclination angle we obtain a mass of $M \approx 12 M_{\odot}$. Additionally, this higher mass fits the fundamental plane as well as timing correlations better than smaller masses. Thus, we use $M = 12 M_{\odot}$.

(ii) *XTE J1118+480*. Belloni et al. (2002b) measured ν_1 for *XTE J1118+480* on the 2000 May 4 and 15. The very large array has

observed the source during that time. We have analysed archival 8.5 GHz data and found a flux of 5.7 mJy on the April 27, 6.4 mJy on the May 13 and 6.8 mJy on the May 31. We interpolate linearly between those dates and estimate the 8.5 GHz flux on the May 4 to be 5.9 mJy and 6.4 mJy on the May 15 and estimate the accretion rate from these radio fluxes. We assume a mass of $6.8 \pm 0.3 M_{\odot}$ (Ritter & Kolb 2003) and a distance of 1.71 ± 0.05 kpc (Chaty et al. 2003).

(iii) *XTE J1550–564*. For the outburst of *XTE J1550–564* in 2002, we use ν_1 values and X-ray fluxes from Belloni et al. (2002a). This outburst never left the hard state. Additionally, we include the outbursts of 1998 and 2000. For these outbursts, we re-analysed the data of the *RXTE* archive to obtain ν_1 . The 2–10 keV X-ray flux has been estimated from the 2–9 keV proportional counter array (PCA) counts assuming that the X-ray spectrum can be described by a power law with photon index of $\Gamma = 1.5$. As the observed X-ray band is similar to the energy range of the estimated flux, the spectral uncertainties do not strongly effect the estimated flux. We assume a distance of 5.3 ± 2.3 kpc (Jonker & Nelemans 2004) and a mass of $10.6 \pm 1 M_{\odot}$ (Orosz et al. 2002).

(iv) *GRO J1655–40*. For *GRO J1655–40*, we reduced public *RXTE* data on MJD 53429.7 to measure ν_1 and obtained the 2–10 keV flux from the spectral model given on the webpage¹ maintained by J. Homan. We assume a mass of $6.3 \pm 0.5 M_{\odot}$ (Greene, Bailyn & Orosz 2001) and a distance of 3.2 kpc (Hjellming & Rupen 1995), but see Foellmi et al. (2006) for significantly lower distance estimates (< 1.7 kpc). We therefore assume 3.2 ± 1.5 kpc.

(v) *GS 1354–644*. For *GS 1354–644*, we assume a mass of $7.34 \pm 0.5 M_{\odot}$ (Casares et al. 2004). The distance to the source is uncertain, Kitamoto et al. (1990) suggest 10 kpc while Casares et al. (2004) give a lower limit of 27 kpc. We will assume a distance of 10 kpc. The 2–10 keV flux and the measurement of ν_1 have been obtained from public *RXTE* data.

(vi) *XTE J1650–500*. *RXTE* started to observe the source during the outburst in 2001 just as the source starts its transition from the hard to the soft state (Homan et al. 2003). We use their first observation which is still in the hard state to obtain a value for ν_1 and the 2–10 keV flux. The distance to *J1650–500* is between 2 and 6 kpc (Tomsick et al. 2003), we assume 4 ± 2 kpc. Orosz et al. (2004) suggest that the BH mass of *J1650–500* is between 4 and $7.3 M_{\odot}$, we use a mass of $5.5 \pm 2 M_{\odot}$.

(vii) *Cyg X-1*. To compare these hard-state measurements with a soft-state object, we also show *Cyg X-1* in its soft state. The high break frequencies are taken from Axelsson, Borgonovo & Larsson (2006). To obtain accretion rates, we use the bolometric luminosities given in Wilms et al. (2006), as soft-state objects are likely to be efficient accretors. The available data have been binned in luminosity bins as described in McHardy et al. (2006). We only include the source for comparison, as the model describing the PSDs for the soft state is different to the Lorentzians we use here. As black hole mass, we use $10 M_{\odot}$, and the distance is assumed to be 2.1 kpc (Massey, Johnson & Degioia-Eastwood 1995).

(viii) *GRS 1915+105*. This source is always accreting at a large fraction of the Eddington accretion rate (Fender & Belloni 2004). It is therefore likely to be efficiently accreting, so we can use the bolometric luminosity to estimate the accretion rate (Körding et al. 2006b). We obtain ν_1 from Belloni et al. (2002b) and X-ray fluxes from Trudolyubov (2001). We assume a mass of $15 M_{\odot}$ and assume the distance to be 11 kpc (Fender et al. 1999; Dhawan, Mirabel &

¹ <http://tahti.mit.edu/opensource/1655/>

Rodríguez 2000; Zdziarski et al. 2005, but see also Chapuis & Corbel 2004; Kaiser et al. 2004 for lower values)

2.3 Neutron stars

For all NSs, we assume a mass of $1.4 M_{\odot}$.

(i) *Low-luminosity X-ray burster*. We include 1E 1724–304, GS 1826–24 and SLX 1735–269 with ν_1 measurements of Belloni et al. (2002b). The 2–10 keV X-ray flux has been obtained from archival *RXTE* PCA data. To obtain the bolometric luminosity and therefore the accretion rate, we use a bolometric correction of 2.5 found for atoll NSs (Migliari & Fender 2006) also for these X-ray burster. We assume distances of 6.6 kpc for 1E 1724–304 (Barbuy, Bica & Ortolani 1998), 5 kpc for GS 1826–24 (Thompson et al. 2005) and 8 kpc for SLX 1735–269 (Molkov et al. 2005).

(ii) *IGR J00291+5934*. The accreting millisecond X-ray pulsar IGR J00291+5934 went into outburst in 2004 (Shaw et al. 2005). Linares, van der Klis & Wijnands (2006) have measured its frequency ν_1 , and we obtain 2–10 keV flux measurements from archival *RXTE* data. As V507 Cas is also in the field of view of the PCA, we assume that the quiescent flux can be attributed to the V507 Cas and subtract this from the measured flux of J00291+5934 during outburst. We assume a distance of 4 kpc (Galloway et al. 2005).

(iii) *Atoll sources*. For the atoll sources, we include 4U 1608–522 with ν_1 measurements from van Straaten, van der Klis & Méndez (2003) (distance of 3.4 kpc; Jonker & Nelemans 2004). The 2–10 keV flux has been estimated from the 3–9 keV PCA count rate assuming a power law with $\Gamma = 1.6$. To obtain a bolometric luminosity, we use a bolometric correction of 2.5. For 4U 1812–12, we use public *RXTE* data to obtain ν_1 measurements and use the bolometric X-ray fluxes from Barret, Olive & Oosterbroek (2003). It should be noted that our measured values for ν_1 are double of those of Barret et al. (2003). We assume a distance of 4 kpc (Cocchi et al. 2000).

(iv) *Z-sources*. We include the Z-sources GX 340 (Jonker et al. 1998, distance of 9.5 kpc) and GX 5–1 (Wijnands et al. 1998, 7.4 kpc). The conversion factor from the 2–16 keV PCA count rate to bolometric luminosity of our Z-sources has been obtained from the Z-source GX 17+2 Di Salvo et al. (2000). The 0.1–200 keV flux given in the paper has been divided by the 2–16 keV PCA counts. For the Z-sources, we use the lower kHz QPO as the frequency ν_1 following Belloni et al. (2002b).

(v) *4U 1728–34*. For 4U 1728–34, Migliari et al. (2005) measure the dependence of ν_h on the radio luminosity and find that it scales with $\nu_h \propto L_{\text{Rad}}^{0.7} \propto \dot{M}$. We include these points for comparison. We assume a distance of 4.6 kpc (Galloway et al. 2003).

2.4 Active galactic nuclei

For AGN, we use the sample presented by Uttley & McHardy (2005). They give the high break frequencies as well as the black hole masses and the bolometric luminosities. The majority of sources are Seyfert galaxies, and thus they are likely high- or very-high-state objects. We can therefore translate the bolometric luminosities directly to accretion rates.

3 RESULTS

For our AGN and the two stellar soft-state BHs, we found in McHardy et al. (2006) that the measured high break frequencies ν_{hb} lie on a plane in the ν_{hb} , \dot{M} and M space:

$$\log \nu_{hb} = \xi_{\text{acc}} \log \dot{M} + \xi_m \log M + b_v, \quad (4)$$

where ξ_{acc} and ξ_m denote the correlation indexes for the accretion rate and the black hole mass; b_v denotes the constant offset. We found that $\xi_{\text{acc}} = 0.98 \pm 0.15$ and $\xi_m = -2.1 \pm 0.15$. Both parameters are within the uncertainties of integer value. We will therefore adopt the integer solution ($\xi_{\text{acc}} = 1$, $\xi_m = -2$) and will not present new fits here.

The edge-on projection of the plane using our sample is shown in Fig. 2. The two lines indicating $\nu_{1,hb} \propto \dot{M} M^{-2}$ ($\nu_{1,hb}$ denotes ν_1 for hard-state objects and ν_{hb} for soft-state objects). The upper line is the fit to soft-state stellar BHs and supermassive BHs using integer valued parameters for the variability plane. For the adopted parameters and our units the constant offset b_v for the soft-state objects is $b_v = -14.5 \pm 0.1$. This offset is different from the one given in McHardy et al. (2006), as we use different units and fixed the parameters of the plane to integer values.

3.1 Stellar black holes

On the left-hand side of Fig. 2, we show the projection of the variability plane ‘zoomed-in’ on our sample of stellar BHs. For hard-state BHs, we have argued that the frequency ν_1 of the lower high-frequency Lorentzian corresponds to the high-frequency break ν_{hb}

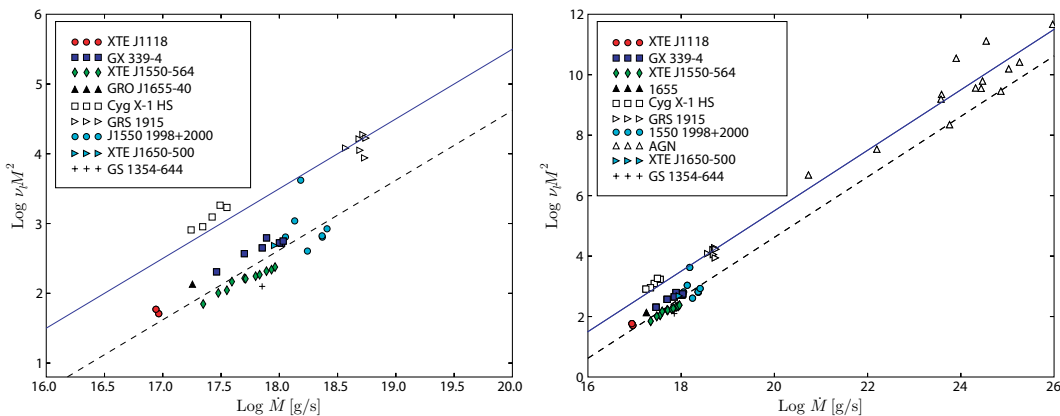


Figure 2. Left-hand side: our sample of stellar BHs. For Cyg X-1 we plot ν_{hb} , while we show ν_1 for the other objects. The lines indicate $\nu_1 \propto \dot{M} M^{-2}$. While the upper line is a fit to soft-state objects (including AGN, see McHardy et al. 2006), the lower is a fit to the hard-state XRBs only. Right-hand side: same as left-hand side, but here, we plot stellar and supermassive objects. In both panels soft-state and IMS objects are plotted with open symbols.

used for soft state. In Fig. 2, we also plot our hard-state BH sample. Similar to the scaling found in soft-state XRBs and AGN, we find that our hard-state BHs follow a scaling $\nu_1 \propto \dot{M}$. However, the constant offset is different for hard- and soft-state objects, and we also show a plane normalized to the hard-state objects only. The constant offset between the soft- and the hard-state scaling is -0.9 dex.

The uncertainties of the measured values shown in Fig. 2 are dominated by systematic errors (e.g. uncertainties in the accretion rate measure) as well as uncertainties of the black hole mass and distance of the BHs. Most uncertainties of all measurements of one source are coupled. Showing these coupled uncertainties as error bars for the data points are therefore misleading. The error budget consists of

(i) *Uncertainties of the primary parameters ν_1 and the radio or X-ray flux.* These uncertainties are different for each data point. A typical value is ≤ 0.04 dex.

(ii) *Uncertainties in the BH mass and distance measurements.* These uncertainties are shared for all data points of a given source. Typical values are between 0.03 and 0.3 dex. This component dominates the total error budget, especially as they enter the variability plane quadratically and our two main sources (GX 339–4 and XTE J1550–564) have large uncertainties in the mass estimate (0.2 and 0.15 dex).

(iii) *Uncertainties of the accretion rate measure.* This uncertainty has two components: First, an uncertainty of the normalization of the accretion rate measure, this would directly change the normalization of all data points. Secondly, uncertainties due to source peculiarities and the individual measurements. The exact value of these uncertainties is hard to access. In Section 2.1, we have argued that their combined effect is roughly ~ 0.2 dex.

The correlation of $\nu_1 \propto \dot{M}$ is found in both hard-state BH that have several measurement (GX 339–4 and XTE J1550–564). The majority of the uncertainties just mentioned do not play a role if one only considers a single source as they would only change the normalization constant b_ν . Thus, we can safely assume that there is a correlation between ν_1 and \dot{M} for individual sources. Whether the constant offset b_ν is significantly different for hard- and soft-state objects need to be verified.

To access the value and uncertainty of the constant offset b_ν for our sample of sources we use two approaches: First, we can compute the direct mean and sample variance of the sources around the correlation using the same weight for all data points. We find $b_\nu = -15.39 \pm 0.04$ with a sample variance of 0.18. However, as many of the errors of the data points are coupled we might underestimate the uncertainty of the mean.

To avoid the coupling of the uncertainties for different data points of a given source, we first treat every source individually and combine the different sources in a second step taking the estimated errors into account. To calculate the error on the mean b_ν , we used the following steps.

(i) Calculate b_ν for each source individually and measure the intrinsic scatter around the linear correlation through the sample variance (σ_{int}).

(ii) Estimate the uncertainty of the measured b_ν for all sources. We set

$$\sigma_b^2 = \sigma_{\text{int}}^2 + (2\sigma_D)^2 + (2\sigma_M)^2 + \sigma_{\dot{M}}^2, \quad (5)$$

where σ_D is the uncertainty of the measurement of the distance, σ_M the mass uncertainty and $\sigma_{\dot{M}}$ the systematic uncertainty of the \dot{M} -measure.

(iii) Calculate that weighted mean and error of mean with the estimated uncertainties. Each source is weighted by their uncertainties and the number of measurements of the source.

Using this method, we find $b_\nu = -15.38 \pm 0.08$. The mean value of b_ν is in agreement with the value found using the sample variance. Finally, we have to consider that the overall normalization of the accretion rate measure has an uncertainty of ~ 0.2 dex. This uncertainty is shared by all data points and all errors in the estimate of the normalization effects the mean value of b_ν directly. If we include this uncertainty we obtain an overall error of 0.22 dex. As the difference between the normalization found for the hard and the soft state is 0.9 dex, we conclude that the difference between the hard- and the soft-state scaling is significant.

Using this method, we can also calculate the expected mean variance of the correlation given the assumed uncertainties. We find $\sigma = 0.38$, which is larger than the sample variance of 0.18. The discrepancy is mainly due to the coupled uncertainties, but we may also have overestimated the uncertainties of the accretion estimator or those of the distance and mass measurements.

Only for GX 339–4 and XTR J1118+480, we have used the radio luminosity to obtain accretion rates while for the other hard-state objects, we used the 2–10 keV flux. We have verified that Fig. 2 does not change significantly if we use the accretion rate measure based on the X-ray flux for all sources. This is not surprising, as the accretion rate measure used for the X-ray flux is partly based on the radio/X-ray correlation of GX 339–4. Thus, our findings are not affected by our choice of different the accretion rate estimators.

The outbursts of XTE J1550–564 in 1998 and 2000 seem to follow a different track than the linear dependence seen in the hard-state outburst in 2002 and the other hard-state objects. The first two outbursts rise more steeply than the linear hard-state scaling. The outbursts seem to start at a frequency ν_1 characteristic for a hard state and lead to values typically found for soft states. In these outbursts the photon index changes strongly during the observations. In 1998, the first observation in our sample has a photon index of $\Gamma = 1.53$ (Sobczak et al. 2000), which changes continuously to the last observation that has $\Gamma = 1.98$, which is atypical for the hard state where one would expect the photon index to stay hard until the state transition. In the 2000 outburst, the source is also softening from $\Gamma = 1.46$ to 1.7 while the power-law cut-off moves from 33 to 19 keV with a significant blackbody component visible in the last observation used (a typical cut-off for the hard state is ~ 80 keV). Thus, it is likely that the source was already in an intermediate state in these outbursts. This suggests that there is one scaling relation for the classical hard state and one with a higher normalization for the soft state, but there is obviously another parameter that governs the transition between those scaling relations. During the transition from the hard to the soft state, the source increases its frequency fast and moves from the hard scaling to the soft one.

For XRBs the transition from the soft to the hard scaling is probably best traced by the spectral index Γ . A strong correlation between timing properties and the photon index has been found in objects near the intermediate states (see e.g. Pottschmidt et al. 2003; Vignarca et al. 2003; Kalemci et al. 2005). A simple dependence on the photon index is however not directly applicable to AGN. The timing properties are also correlated to the hardness ratio (see e.g. Belloni et al. 2005). The hardness ratio can be generalized to the non-thermal fraction $f = \frac{L_{\text{PL}}}{L_{\text{Disc}} + L_{\text{PL}}}$, where L_{Disc} is the luminosity in the multicolour blackbody component while L_{PL} describes the luminosity of the power-law component. This

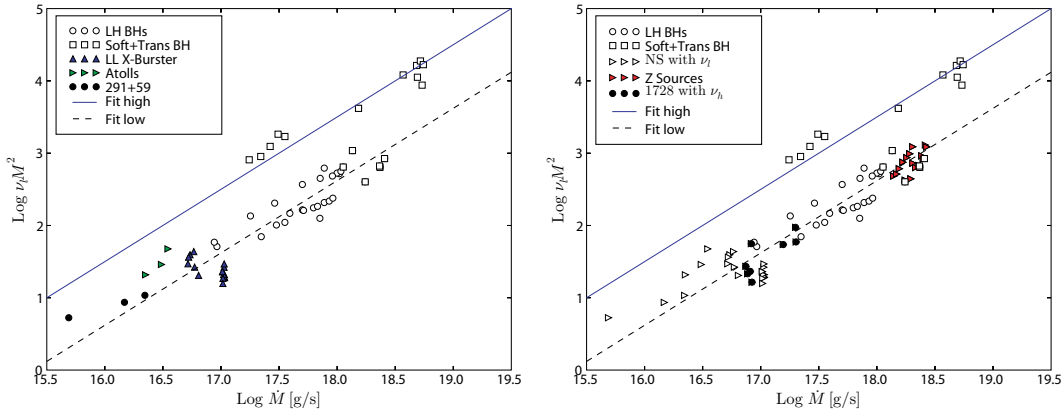


Figure 3. Left-hand panel: NSs with measured ν_1 in comparison with our stellar BH sample. The NS sample seems to follow the correlation, albeit with larger scatter. The upper line shows the correlation normalized to soft-state objects while the lower line is normalized for hard-state objects. Right-hand panel: inclusion of kHz QPOs of Z-sources. While the kHz QPOs of Z-sources are near the correlation this is not true for kHz QPOs of atoll sources (see the text for a detailed discussion).

non-thermal fraction has similar properties as the hardness ratio but is also applicable to AGN (see Körding, Jester & Fender 2006c). Sources solidly in the soft-state ($f = 0$) follow a track given by $\log \nu_{1,\text{hb}} = \log(\dot{M}M^{-2}) - 14.7$, while those in the hard-state ($f = 1$) follow $\log \nu_{1,\text{hb}} = \log(\dot{M}M^{-2}) - 14.7 - 0.9$. In the transition between both the states, the frequencies depend on the photon index and therefore on f . This suggests that the dependence of ν on M , \dot{M} and f can be approximated by

$$\log \nu_{1,\text{hb}} = \log \dot{M} - 2 \log M - 14.7 - 0.9 \theta(f), \quad (6)$$

where θ is a monotonic function with $\theta(0) = 0$ and $\theta(1) = 1$. Unfortunately, with the readily available data of state transitions we are not able to fully constrain it. We note that this dependence may have to be further modified due to hysteresis effects similar to those seen in hardness-intensity diagrams.

3.2 Neutron stars

In the left-hand panel of Fig. 3, we show our sample of NSs with visible broad lower high-frequency Lorentzians (L_1) together with the stellar BHs. The low-luminosity X-ray burster and the accreting millisecond pulsar lie near the expected scaling for hard-state BHs – but with increased scatter. Also, our atoll sources are in a similar frequency range. However, while we could observe the linear dependency of ν_1 on accretion rate in some single sources for BHs (i.e. XTE J1550–564 and GX 339–4) this is harder for the NSs, since the accretion rate changes in our sample are small. The only object changing its accretion rate significantly is IGR J00291+5934. For that source, the slope seems to be slightly shallower than what is found for the BHs. However, as already mentioned, a second source (V507 Cas) is in the field of view of the PCA, so it is hard to measure correct fluxes for the pulsar. It may be that we are underestimating the lowest detected fluxes. As a sample the NS sources still scatter around the correlation found for hard-state BHs, albeit with a larger scatter.

Psaltis et al. (1999) present a tight correlation between the frequencies of the low-frequency QPO (ν_{LF}) and those of the lower kHz QPO in NSs and BHs. In the unified picture of Belloni et al. (2002b) the lower kHz QPO found in some NSs is identified with the broad lower high-frequency Lorentzian L_1 for BHs and weakly accreting NSs. As the correlation between ν_1 and $\dot{M}M^{-2}$ holds for some sources on the ν_{LF}/ν_1 correlation, it may be possible that one

can extend our accretion rate ν_1 correlation to all sources on the Psaltis et al. (1999) correlation.

We have just shown that atoll sources with a measured frequency ν_1 roughly follow the variability plane. At higher accretion rates atoll sources show a lower kHz QPO at significantly higher frequencies than the observed values of ν_1 at low accretion rates (when the lower kHz QPO is observed the broad lower high-frequency Lorentzian L_1 is not seen). However, the increase in the accretion rate is not sufficient to ensure that the lower kHz QPO is in agreement with the correlation. This can also be shown by looking at ν_h for 1728–34. ν_h is the frequency corresponding to the broad ‘hump’ Lorentzian (L_h) of the low-frequency QPO. Thus, ν_h and the frequency of the low-frequency QPO are well correlated and have roughly similar values. As we show on the right-hand side of Fig. 3, ν_h is (at least for 1728) near the correlation. Thus, the lower kHz QPO will be above the correlation by a factor of ~ 15 .

Z-sources have significantly higher accretion rates than atoll sources and often show kHz QPOs. The frequencies of the lower kHz QPOs of Z-sources are shown in Fig. 3. The accretion rates are so large that the frequencies of the lower kHz QPO of Z-sources are near the hard-state correlation. However, Z-sources are very strongly accreting, for example, they belong to a bright IMS. These sources should therefore follow the high-state slope similar to the BH GRS 1915+105. The lower kHz QPO frequencies are so high that they have the same order of magnitude as the Keplerian frequency at the surface of the NS (~ 1700 Hz). Thus, it may be that the frequencies start to saturate and are therefore slightly below the high-state correlation. See also the discussion on WD and the corresponding Fig. 6 where this effect may be even more pronounced.

The slope of the Z-sources alone seems to be steeper than the correlation found for BHs. It may be that while the accretion rate does not change very much the sources make a state transition from the analogue of the hard IMS to the soft IMS (horizontal branch to normal branch). As we have seen for BHs, during state transitions the source moves rapidly from the hard-state scaling to the soft-state scaling. This rapid transition explains the steeper slope of Z-sources. Nevertheless, as the kHz QPOs of atoll sources do not fit on the correlation we cannot be sure if it is not pure coincidence that the Z-sources seem to follow the correlation. For the correlation, we therefore have to rely on sources with measured ν_1 .

We have mentioned in the introduction that the ‘parallel tracks’ found in flux frequency diagrams may suggest that the frequency of

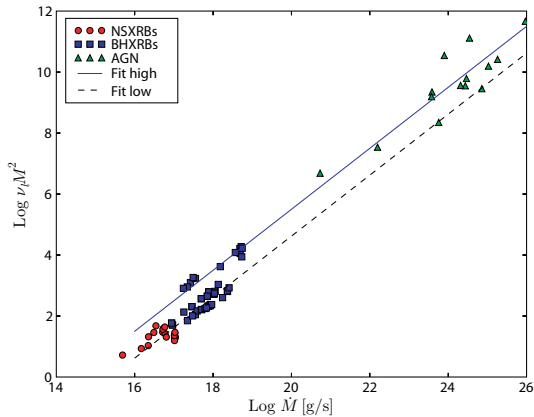


Figure 4. Edge-on projection of the variability plane including AGN, stellar BHs and NSs with directly measured ν_1 .

the kHz QPO may be a better tracer of the instantaneous accretion rate than the X-ray luminosity (van der Klis 2001). We are currently unable to use any frequency as a direct tracer of the accretion rate as the conversion factors are yet unknown. As we have shown, it is likely that the frequency (ν_1) does depend not only on the accretion rate but also on the state of the source. Thus, at least ν_1 cannot be used as a measure of the accretion rate for all times if one does not have detailed information on the state of the source. If the frequency of the lower high-frequency Lorentzian does depend not only on the accretion rate but also on an additional parameter describing the accretion state, one could explain the parallel tracks. On short time-scales the main parameter is either the accretion rate or the accretion rate and the accretion state parameter are strongly coupled creating the well-correlated tracks. On longer time-scales the relationship of the two parameters can change so that one observes parallel tracks.

The final edge-on projection of the variability plane including BH XRBs, NS XRBs with directly measured ν_1 and AGN is shown in Fig. 4. As a sample the NSs extend the correlation towards lower accretion rates.

3.3 Comments on DNOs for accreting WDs

The aforementioned correlation of the frequencies of the LF QPOs with those of the lower kHz QPO (Psaltis et al. 1999) has also been extended to include CVs (e.g. Warner et al. 2003). Here, the DNO frequency corresponds to the frequency ν_1 of the lower high-frequency Lorentzian. In Table 1, we tabulate the parameters of four well-known systems.

Table 1. Parameters of our WD sample.

	\dot{M} (g s^{-1})	ν_{DNO} (Hz)	$\log \nu M^2$	$(\log \nu M^2)_{\text{pred}}$
IX Vel	5×10^{17}	3.7×10^{-2}	-1.62	3
UX UMa	4×10^{17}	3.4×10^{-2}	-1.56	2.9
OY Car	3×10^{16}	5.5×10^{-2}	-1.59	1.8
VW Hyi	$\gtrsim 6 \times 10^{14}$	$\sim 1 \times 10^{-2}$	-2.1	0.1

Masses: IX Vel: $0.8 M_{\odot}$, UX UMa: $0.9 M_{\odot}$, OY Car: $0.69 M_{\odot}$ and VW Hyi: $0.84 M_{\odot}$. References: IX Vel: Beuermann & Thomas (1990), UX UMa: Froning, Long & Knigge (2003), Suleimanov et al. (2004), Baptista et al. (1998), Knigge et al. (1998), OY Car: Marsh & Horne (1998), Pratt et al. (1999), Wood et al. (1989), VW Hyi: Warner & Woudt (2006), Pandel, Córdova & Howell (2003), Sion et al. (1997).

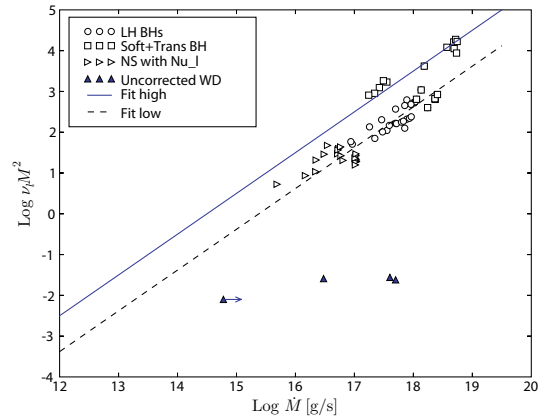


Figure 5. Edge-on projection of the variability plane compared to our sample of WDs. The uncertainty on the accretion rates in a factor of 2–3, so in logspace 0.3–0.5 dex.

The accretion rates of CVs have higher uncertainties than those of NSs or BHs, as the majority of the bolometric luminosity is not emitted in the well-accessible X-ray band. We assume that the accretion rates are only correct up to a factor of 2–3. Especially, the accretion rate for VW Hyi is uncertain, as we use the quiescent value as a lower limit to the accretion rate, while the DNO frequencies are measured during the end of the decline from an outburst. Thus, the accretion rate will be approximately the quiescent rate. Nevertheless, observed values of $\log \nu M^2$ are mostly around -1.6 , while we expect values between 0.1 and 3 (assuming that they follow the soft-state scaling). Thus, in the current form, the correlation is not valid for CVs (see Fig. 5). We note that, for CVs, the DNO frequency rises with accretion rate (Woudt & Warner 2002), similar to the expected behaviour of the correlation.

However, up to now we have not considered that a WD is significantly larger than a NS or a BH. It is not evident how to correct the correlation for the larger radius. For BHs the radius is linearly related to the BH mass. Thus, the correlation found for BHs suggests that one or both mass terms of the correlation correspond to a radius. If one of the mass terms corresponds to a radius, the correlation reads $\nu_1 \propto \frac{\dot{M}}{MR}$, where R is the radius of the central object. This correlation can be read as a correlation between ν_1 and the power liberated in the accretion disc around the central object divided by M^2 . The power liberated in a standard accretion disc around a central object with radius R is $R/(6GM/c^2)$ times smaller than the power liberated in a disc around a non-rotating BH, the one radius term corrects for this fact. A WD of average mass has a radius roughly ~ 500 times larger than that of a NS. This would move the expected position of OY Car and VW Hyi near our correlations (see Fig. 6). Their positions are in agreement with the correlation given the large uncertainties on the accretion rates. IX Vel and UX UMa, however, are still far from the correlation. Those two sources are nova-likes, with high accretion rates. If the correlation would hold for all those sources, their frequencies would exceed the break-up frequency of the WD (~ 5) Hz. If the DNO frequency (or ν_1) is somehow related to the Keplerian rotation this is impossible. Thus, it is likely that the sources follow the correlation until the frequencies are comparable to the fastest possible frequency (break-up frequency for WDs and the frequency of the innermost stable orbit for BHs). For these high accretion rates the frequencies cannot increase any further and stay constant around the fastest possible frequency. Schematic frequency tracks for WDs, BHs and NSs are shown in Fig. 6. The shown lines should only

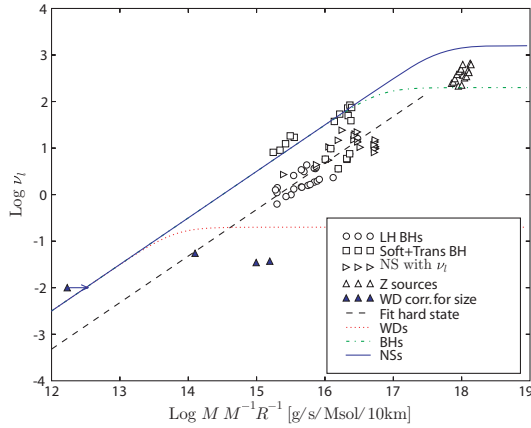


Figure 6. Projection of the variability plane on to the $\nu_1 \frac{\dot{M}}{MR}$ plane. Besides the scaling relation expected for hard-state objects, we also show the break-up frequency of WDs (~ 5 Hz) and NSs (~ 1700 Hz) and the frequency at the innermost stable orbit of BHs (~ 240 Hz). Sources can only follow the correlation until the frequencies are comparable to the break-up frequency, there the correlation needs to level-off to the constant break-up frequency.

illustrate possible frequency tracks. As the break-up frequencies are reached at high luminosities the shown tracks are normalized to the high-state correlation. The shown function is a smooth broken power law which is linear with \dot{M} at low accretion rates and constant at high accretion rates $\{\nu \propto \dot{M}[1 + (\dot{M}/\dot{M}_0)^2]^{-0.5}\}$. If one assumes that both mass terms of the correlation correspond to radii, none of the measured WDs fall on the expected correlation. Thus, we consider it to be more likely that only one mass term corresponds to a radius. In summary, while dwarf novae systems seem to lie near the correlation if one takes the size of the central object into account, nova-like objects do not seem to follow the correlation as their frequencies would exceed the break-up frequency of the WD.

4 DISCUSSION

In the previous section, we found that the variability plane found in soft-state accreting BHs (McHardy et al. 2006) can be extended to hard-state stellar BHs (see Fig. 2). The frequencies depend on the accretion rate (\dot{M}) and the black hole mass (M) as

$$\left(\frac{\nu_1}{\text{Hz}}\right) \left(\frac{M}{10 M_\odot}\right) \approx 2.2 \left(\frac{\dot{M}}{0.01 \dot{M}_{\text{Edd}}}\right), \quad (7)$$

for soft-state objects; for hard-state objects the proportionality factor is ~ 0.3 . It is even possible to extend the correlation to NS with directly measured frequencies ν_1 (see Fig. 4). Here, we discuss the physical implications of these findings.

This dependence on the accretion rate as well as on the black hole mass can be simplified by assuming that the accreting BH is scale invariant (e.g. Merloni et al. 2003; Falcke et al. 2004). If the frequency arises through Keplerian motion or any other process scaling with the size of the central object, the left-hand side of the equation is invariant of black hole mass. The right-hand side denotes a simple linear dependence on the accretion rate in Eddington units.

While a linear dependency on the accretion rate is seen if a source is in the canonical hard or soft state this is not the case for sources in intermediate states or near the state transition. For example, we have seen that XTE J1550–564 follows the linear scaling in its hard outburst in 2002, while the frequencies rise faster than linear

for the other outbursts. Thus, besides accretion rate there must be at least a second parameter governing the observed frequencies (ν_1 , ν_{hb}). Similar to the hysteresis found for state changes (see e.g. the hardness intensity diagrams of XRB outbursts), there seems to be a hysteresis effect for the frequencies (see fig. 7 in Belloni et al. 2005).

In case the high-frequency break originates from Keplerian motion or a frequency that is related to the Keplerian frequency, we can use equation (7) to obtain the dependence of the active radius r_a , which corresponds to the break in the PSD, on the accretion rate. This yields

$$\frac{r_a}{R_G} = 625 \left(\frac{\dot{M}}{0.01 \dot{M}_{\text{Edd}}}\right)^{-2/3}, \quad (8)$$

where R_G is the gravitational radius $R_G = GM/c^2$. The correlation with the accretion rate therefore implies that the radius associated with the break moves inwards with $\dot{M}^{-2/3}$. Interestingly, such a behaviour may be observed in GRS 1915+105. Belloni et al. (1997) report that the disc radius associated with the region emitting the measured X-ray spectrum changes from 70 km to roughly 20 km while the *RXTE/PCA* count rate increases by a factor of ~ 5 . If the bolometric correction does not change significantly between the different observations, this suggests that the emitting radius moves inwards as $r^{-0.75}$ compared to our prediction of $r^{-0.67}$.

It is tempting to associate the active region creating the high-frequency break with the transition from the geometrically thin standard disc to the optically thin inefficient accretion flow. However, most of our objects are soft-state objects. Within the soft state it is usually assumed that the optically thick, geometrically thin accretion disc reaches up to the last stable orbit. The luminosities of a given source in the soft state can change by a factor of 15 (2–30 per cent Eddington), so the inner disc radius would have to change by a factor of 6. This is not in agreement with the radii deduced from X-ray spectral fitting nor with observed scaling of the X-ray luminosities with disc temperature as T^4 (e.g. Gierliński & Done 2004). Furthermore, the observed frequencies are far too low to originate from a Keplerian motion at the inner edge of the accretion disc (innermost stable orbit). We further note that for a normal standard disc, viscous time-scales are too long (~ 2 s) to explain the high frequencies and seem to have a very low dependency on accretion rate ($\alpha^{-4/5} M^{-3/10}$). It may well be that the break frequency is indeed associated with a Keplerian motion. However, as we have argued, the corresponding radius does not seem to be directly associated with the inner edge of the standard disc. Maybe this radius only reaches the innermost radii for highly accreting objects like Z-sources with their lower kHz QPO.

We have seen that NSs with measured ν_1 seem to follow the suggested correlation. At higher accretion rate the Z-sources have lower frequencies than expected. This discrepancy may arise from the slightly larger size of the NS with its boundary layer compared to a BH with similar mass. While increasing the accretion rate, the emitting region cannot move inwards as expected as it is stopped by the boundary layer. This may also be the reason for the relatively low DNO frequencies of strongly accreting WDs (see Fig. 6).

5 CONCLUSION

We have shown that the variability plane found in AGN and soft-state XRBs ($\nu_{\text{hb}} M \propto \dot{M}/\dot{M}_{\text{Edd}}$) can be extended to hard-state BH XRBs and weakly accreting NSs. For hard-state objects the frequency of the lower high-frequency Lorentzian (ν_1) corresponds to

the high-frequency break in AGN and soft-state XRBs. For WDs, the situation seems to be more complicated as we need to correct for the WD radius. While some dwarf novae seem to lie near the correlation (within the large uncertainties), strongly accreting nova-like systems do not seem to follow the correlation as the frequencies would otherwise exceed the break-up frequency of the WD. In case that the high break frequency in the PSD is related to a Keplerian orbit around the BH, we find that this radius in gravitational radii depends on the accretion rate as $(\dot{M}/\dot{M}_{\text{Edd}})^{-2/3}$. However, the orbit corresponding to the high break is unlikely to be directly related to the radius where the standard optically thick disc turns into an optically thin inefficient accretion flow.

ACKNOWLEDGMENTS

We thank Tom Maccarone for helpful discussions. We are grateful for constructive comments by our referee. EGK acknowledges funding via a Marie Curie Intra-European Fellowship under contract no. MEIF-CT-2006-024668. EGK would like to thank J. Wilms for discussions on a related subject.

REFERENCES

- Axelsson M., Borgonovo L., Larsson S., 2006, *A&A*, 452, 975
 Baptista R., Horne K., Wade R. A., Hubeny I., Long K. S., Rutten R. G. M., 1998, *MNRAS*, 298, 1079
 Barbuy B., Bica E., Ortolani S., 1998, *A&A*, 333, 117
 Barret D., Olive J. F., Oosterbroek T., 2003, *A&A*, 400, 643
 Belloni T., Mendez M., King A. R., van der Klis M., van Paradijs J., 1997, *ApJ*, 488, L109
 Belloni T., Colombo A. P., Homan J., Campana S., van der Klis M., 2002a, *A&A*, 390, 199
 Belloni T., Psaltis D., van der Klis M., 2002b, *ApJ*, 572, 392
 Belloni T., Homan J., Casella P., van der Klis M., Nespoli E., Lewin W. H. G., Miller J. M., Méndez M., 2005, *A&A*, 440, 207
 Beuermann K., Thomas H.-C., 1990, *A&A*, 230, 326
 Casares J., Zurita C., Shahbaz T., Charles P. A., Fender R. P., 2004, *ApJ*, 613, L133
 Chappuis C., Corbel S., 2004, *A&A*, 414, 659
 Chaty S., Haswell C. A., Malzac J., Hynes R. I., Shrader C. R., Cui W., 2003, *MNRAS*, 346, 689
 Cocchi M., Bazzano A., Natalucci L., Ubertini P., Heise J., Kuulkers E., in't Zand J. J. M., 2000, in McConnell M. L., Ryan J. M., eds, *AIP Conf. Ser. Vol. 510, The Fifth Compton Symposium*. Springer, Berlin, p. 217
 Cui W., Zhang S. N., Focke W., Swank J. H., 1997, *ApJ*, 484, 383
 Dhawan V., Mirabel I. F., Rodríguez L. F., 2000, *ApJ*, 543, 373
 Di Salvo T. et al., 2000, *ApJ*, 544, L119
 Edelson R., Nandra K., 1999, *ApJ*, 514, 682
 Esin A. A., McClintock J. E., Narayan R., 1997, *ApJ*, 489, 865
 Falcke H., Körding E., Markoff S., 2004, *A&A*, 414, 895
 Fender R., Belloni T., 2004, *ARA&A*, 42, 317
 Fender R. P., Garrington S. T., McKay D. J., Muxlow T. W. B., Pooley G. G., Spencer R. E., Stirling A. M., Waltman E. B., 1999, *MNRAS*, 304, 865
 Foellmi C., Depagne E., Dall T. H., Mirabel I. F., 2006, *A&A*, 457, 249
 Ford E. C., van der Klis M., Méndez M., Wijnands R., Homan J., Jonker P. G., van Paradijs J., 2000, *ApJ*, 537, 368
 Froning C. S., Long K. S., Knigge C., 2003, *ApJ*, 584, 433
 Galloway D. K., Psaltis D., Chakrabarty D., Muno M. P., 2003, *ApJ*, 590, 999
 Galloway D. K., Markwardt C. B., Morgan E. H., Chakrabarty D., Strohmayer T. E., 2005, *ApJ*, 622, L45
 Gierliński M., Done C., 2004, *MNRAS*, 347, 885
 Green A. R., McHardy I. M., Lehto H. J., 1993, *MNRAS*, 265, 664
 Greene J., Bailyn C. D., Orosz J. A., 2001, *ApJ*, 554, 1290
 Hjellming R. M., Rupen M. P., 1995, *Nat*, 375, 464
 Homan J., Belloni T., 2005, *Ap&SS*, 300, 107
 Homan J., Klein-Wolt M., Rossi S., Miller J. M., Wijnands R., Belloni T., van der Klis M., Lewin W. H. G., 2003, *ApJ*, 586, 1262
 Hynes R. I., Steeghs D., Casares J., Charles P. A., O'Brien K., 2003, *ApJ*, 583, L95
 Hynes R. I., Steeghs D., Casares J., Charles P. A., O'Brien K., 2004, *ApJ*, 609, 317
 Jonker P. G., Nelemans G., 2004, *MNRAS*, 354, 355
 Jonker P. G., Wijnands R., van der Klis M., Psaltis D., Kuulkers E., Lamb F. K., 1998, *ApJ*, 499, L191
 Kaiser C. R., Gunn K. F., Brocksopp C., Sokoloski J. L., 2004, *ApJ*, 612, 332
 Kalemci E., Tomsick J. A., Buxton M. M., Rothschild R. E., Pottschmidt K., Corbel S., Brocksopp C., Kaaret P., 2005, *ApJ*, 622, 508
 Kitamoto S., Tsunemi H., Pedersen H., Ilovaisky S. A., van der Klis M., 1990, *ApJ*, 361, 590
 Knigge C., Drake N., Long K. S., Wade R. A., Horne K., Baptista R., 1998, *ApJ*, 499, 429
 Körding E., Falcke H., Corbel S., 2006a, *A&A*, 456, 439
 Körding E. G., Fender R. P., Migliari S., 2006b, *MNRAS*, 369, 1451
 Körding E. G., Jester S., Fender R., 2006c, *MNRAS*, 372, 1366
 Linares M., van der Klis M., Wijnands R., 2007, *ApJ*, 660, 595
 Markowitz A. et al., 2003, *ApJ*, 593, 96
 Marsh T. R., Horne K., 1998, *MNRAS*, 299, 921
 Massey P., Johnson K. E., Degioia-Eastwood K., 1995, *ApJ*, 454, 151
 McClintock J., Remillard R., 2006, in Lewin W. H. G., van der Klis M., eds, *Compact Stellar X-ray Sources*. Cambridge Univ. Press, Cambridge
 McHardy I., 1988, *Memorie della Societa Astronomica Italiana*, 59, 239
 McHardy I. M., Koerding E., Knigge C., Uttley P., Fender R. P., 2006, *Nat*, 444, 730
 Merloni A., Heinz S., Di Matteo T., 2003, *MNRAS*, 345, 1057
 Migliari S., Fender R. P., 2006, *MNRAS*, 366, 79
 Migliari S., Fender R. P., van der Klis M., 2005, *MNRAS*, 363, 112
 Molkov S., Revnivtsev M., Lutovinov A., Sunyaev R., 2005, *A&A*, 434, 1069
 Nowak M. A., 1995, *PASP*, 107, 1207
 Orosz J. A. et al., 2002, *ApJ*, 568, 845
 Orosz J. A., McClintock J. E., Remillard R. A., Corbel S., 2004, *ApJ*, 616, 376
 Pandel D., Córdova F. A., Howell S. B., 2003, *MNRAS*, 346, 1231
 Pottschmidt K. et al., 2003, *A&A*, 407, 1039
 Pratt G. W., Hassall B. J. M., Naylor T., Wood J. H., Patterson J., 1999, *MNRAS*, 309, 847
 Psaltis D., Belloni T., van der Klis M., 1999, *ApJ*, 520, 262
 Ritter H., Kolb U., 2003, *A&A*, 404, 301
 Shahbaz T., Fender R., Charles P. A., 2001, *A&A*, 376, L17
 Shaw S. E. et al., 2005, *A&A*, 432, L13
 Sion E. M., Cheng F. H., Sparks W. M., Szkody P., Huang M., Hubeny I., 1997, *ApJ*, 480, L17
 Sobczak G. J., McClintock J. E., Remillard R. A., Cui W., Levine A. M., Morgan E. H., Orosz J. A., Bailyn C. D., 2000, *ApJ*, 544, 993
 Suleimanov V. F., Neustroev V. V., Borisov N. V., Fioktistova I. S., 2004, in Tovmassian G., Sion E., eds, *Rev. Mex. Astron. Astrofis. Conf. Ser., Time-Resolved Spectroscopy and Doppler Tomography of UX UMA*. Instituto de Astronomia, UNAM, p. 270
 Tomsick J. A., Kalemci E., Corbel S., Kaaret P., 2003, *ApJ*, 592, 1100
 Thompson T. W. J., Rothschild R. E., Tomsick J. A., Marshall H. L., 2005, *ApJ*, 634, 1261
 Trudolyubov S. P., 2001, *ApJ*, 558, 276
 Uttley P., McHardy I. M., 2005, *MNRAS*, 363, 586
 Uttley P., McHardy I. M., Papadakis I. E., 2002, *MNRAS*, 332, 231
 van der Klis M., 2001, *ApJ*, 561, 943
 van Straaten S., van der Klis M., Méndez M., 2003, *ApJ*, 596, 1155
 Vignarca F., Migliari S., Belloni T., Psaltis D., van der Klis M., 2003, *A&A*, 397, 729

Warner B., Woudt P. A., 2006, MNRAS, 367, 1562

Warner B., Woudt P. A., Pretorius M. L., 2003, MNRAS, 344, 1193

Wijnands R., Mendez M., van der Klis M., Psaltis D., Kuulkers E., Lamb F. K., 1998, ApJ, 504, L35

Wilms J., Nowak M. A., Pottschmidt K., Pooley G. G., Fritz S., 2006, A&A, 447, 245

Wood J. H., Horne K., Berriman G., Wade R. A., 1989, ApJ, 341, 974

Woudt P. A., Warner B., 2002, MNRAS, 333, 411

Zdziarski A. A., Gierliński M., Rao A. R., Vadawale S. V., Mikołajewska J., 2005, MNRAS, 360, 825

This paper has been typeset from a $\text{T}_{\text{E}}\text{X}/\text{L}^{\text{A}}\text{T}_{\text{E}}\text{X}$ file prepared by the author.